Influence of *p*H on the formation of a polyelectrolyte complex by dissipative particle dynamics simulation: From an extended to a compact shape

Efrain Meneses-Juárez,[1,2] César Márquez-Beltrán,[1] and Minerva González-Melchor[1,*]

[1]*Instituto de Física "Luis Rivera Terrazas," Benemérita Universidad Autónoma de Puebla, Apartado Postal J-48, Puebla 72570, Mexico*

[2]*Facultad de Ciencias Básicas, Ingeniería y Tecnología, Universidad Autónoma de Tlaxcala, Calzada Apizaquito S/N, Apizaco, Tlaxcala 90300, Mexico*

(Received 26 February 2019; revised manuscript received 28 May 2019; published 31 July 2019)

This work aims to investigate the influence of *p*H on the mechanism of assembly of macromolecules. We studied the effect of the *p*H on the interaction of two polyelectrolytes of opposed charge, having the same size, by means of dissipative particle dynamics method. The system consisted of a strong cationic and a weak anionic polyelectrolyte in an aqueous solution containing monovalent counterions. The analysis was made by varying the *p*H of the solution, which modifies the charge fraction of the weak anionic polyelectrolyte with a dissociation acid constant *p*Ka of 5.5, while the polycation is fully charged in all the *p*H range used, characteristic of a strong polyelectrolyte. In order to describe the influence of *p*H on the complexation process, we have analyzed the pair radial distribution functions polyanion-counterion, polycation-counterion, and polyanion-polycation. The complex conformation was studied by means of the radius of gyration and the end-to-end distance of both chains as the *p*H varied from 1 to 14. A relevant finding obtained here was the relationship between the radial distribution functions and the counterion release from the polyelectrolytes, which leads to a reduction in the size of the complex when *p*H increased. Surprisingly, a transition from an extended to a compact polyelectrolyte complex was obtained when the *p*H reached the dissociation acid constant *p*Ka of the weak polyelectrolyte. This systematic study can help to understand a large number of more realistic problems in biological systems such as protein complex, chromatin phase transition, or in complex systems applied in biomedical science.

DOI: 10.1103/PhysRevE.100.012505

I. INTRODUCTION

Currently, it is possible to synthesize copolymers made of monomers with and without charge and even to vary their charge fraction [1]; in this process the total number of charged groups and their positions along the chain are imposed by the chemical reactions. The assembly of individual proteins and their complex structure is fundamental in every biological process; in these systems the conformational changes of the macromolecules can be originated by variations in the solvent, amount of salt, variations in *p*H, temperature, etc., which in turn change biofunctional processes [2]. A fundamental feature in biological systems is the compaction of DNA and its packaging in living cells [3]. Recent studies have shown that the mixture of DNA and polyethylene glycol-polyphosphoramidate (PEG-PPA) block copolymer in solvents with different polarities produces the assembly of micellar nanoparticles with different shapes, ranging from worm and rodlike structures to spheroidal shapes [4]. Another example is the complexation between polyamines and DNA, where the interaction occurs through electrostatics. Being the polyamide the one that presents positive charge, its mixing with DNA results in aggregation [5], compaction [6], and precipitation [7]. Indeed, in this type of biological assembly, steric, electrostatic, hydration, and hydrophobic interactions play a very important role on the final structure. If the interacting species are two oppositely charged polymers, the resulting aggregate is known as a polyelectrolyte complex [8,9].

Polyelectrolyte complexes (PECs) have revealed that electrostatic interactions between oppositely charged groups are the leading factors in controlling the complex formation and its structure [10–12]. Polyelectrolytes are classified by their ability to ionization in water as strong and weak. Strong polyelectrolytes are easily ionized, and their electrostatic charge is not too sensitive to the *p*H of the solution. In contrast, weak polyelectrolytes are very sensitive to *p*H changes because ionic equilibrium determines the ionization of their anionic or cationic groups [9]. It has been found that depending on the interacting polyelectrolytes and the environmental conditions it is possible to obtain different chain conformations. For instance, for very strong electrostatic interactions, PECs often show dense glasslike structures with distinct round surface and pronounced local order.

The formation of polyelectrolyte complexes is an important phenomenon that has not been well understood. The self-assembly of PECs is relatively difficult since they are very sensitive to the ionic strength and the mixing ratio of polyelectrolytes such as Dautzemberg found in his research using sodium polystyrene sulfonate (PSS) as polyanion and polydiallyl dimethylammonium chloride as the polycation [13]. In his study, very small amounts of sodium chloride (NaCl) lead to a drastic decrease of the level of aggregation, while higher ionic strength results in macroscopic flocculation (or coacervation). However, not only salt concentration or mixing ratio affect the structural behavior of the PECs; for

*Corresponding author: minerva@ifuap.buap.mx

example, Mengarelli *et al.* [14] found that the phase behavior of polyelectrolyte complexes formed by mixing polymethacrylic acid and polyethyleneimine shows two distinct regimes: weak and strong complexation, which appear successively as *p*H increases. Here, the polymethacrylic acid is weakly dissociated, whereas polyethyleneimine is strongly protonated.

On the other hand, it is very well known that while an uncharged linear polymer chain is usually found in a random conformation in solution (closely approximating a self-avoiding three-dimensional random walk), the charges on a linear polyelectrolyte chain will repel each other due to Coulomb repulsion, which causes the chain to adopt a more expanded conformation. If the solution contains a great amount of added salt, the charges will be screened and, consequently, the polyelectrolyte chain will collapse to a more conventional conformation (essentially identical to a neutral chain in good solvent). On the other hand, for strongly charged polyelectrolytes, the nature of counterion (multivalent counterions) can play an important role on the charge of the chain due to ion condensation phenomena [15]. Thus, the structure and morphology of the formed polyelectrolyte complex when an ionic strength is applied into the solution can be understood in terms of the conformation of the polyelectrolyte chains before mixing. However, the strong increase in the complex diameter at higher ionic strength is related to the screening phenomenon. A very important review that presents selected ideas concerning complexes formed by oppositely charged polyelectrolytes was made by Thünemann *et al.* [16]

Márquez-Beltrán *et al.* [17] have found that a system composed by PSS and polyallylamine hydrochloride (PAH) exhibits a primary aggregation, such as in a dispersed colloidal system, and a secondary high aggregation when NaCl concentration increases above 1.0 M, which is almost 10 times higher than that used by other authors for other types of polyelectrolytes [13]. It suggests that the level of aggregation can be better controlled for systems containing weak and strong polyelectrolytes. In Márquez-Beltrán's studies, the complex formation was also dependent on the *p*H, given that the aggregation found is higher for the basic solution as compared with the acidic solutions. In a previous paper [18], we simulated a two-chain PSS/PAH system using dissipative particle dynamics simulations [19]. In that study, we analyzed the influence of both the ionic strength (*monovalent salt*) and the molar mixing ratio on the complex formation mechanism. Our findings showed a conformational change of the complex. The discussion was focused on the variation of conformation of each chain and on the release of their counterions. In addition, other computer experiments showed that PECs formed by a long stiff macroion and a few relatively short oppositely charged flexible macromolecules can display toroidal, rod, and tennis racket structures [20,21]. Furthermore, Petrov *et al.* [22] studied the mixing of two polyelectrolytes of opposed charge in solution either in water with or without a NaCl concentration; their findings show that an anticooperative character of proton binding at base-acid titration of free PAH changes to a highly cooperative process in the presence of PSS.

On the other hand, computer simulation techniques have critically influenced the investigation on different aspects of soft condensed matter systems, and polyelectrolyte complexation is not an exception since these powerful tools allow the exploration of the physics behind these phenomena in a very controlled and systematic way. Simulation techniques range from *ab initio* quantum mechanical calculations, atomistic molecular dynamics and Monte Carlo methods, coarse-grained descriptions, and continuum approaches. At atomistic level, the computer requirements increase considerably if solvent molecules are explicitly included in the calculations [23]. Although very important advances in coding, speed of processing, high performance computer architectures and algorithms have been achieved (for example, the first billion-atom biomolecular simulation was recently announced [24]), the explicit inclusion of solvent molecules is still one of the biggest challenges for everyday calculations. So, a common approach is to take solvent effects implicitly, for instance, in Brownian dynamics the solvent is included via the viscosity of the medium in the friction force. An alternative approach is to consider a coarse-grained model where several atoms are grouped into a single coarse-grained bead [25]. In this way, three or more water molecules become one solvent bead, an ion with its hydration shell becomes a pseudoion, and so on. The key point in these coarse-grained models is the parametrization of the effective interaction potentials, which frequently requires previous all-atom simulations. In going from the atomistic to the coarse-grained level, some resolution would be lost at some degree but the gap between the simulated time and length scales and the experimental measurements would be shortened. Hoogerbrugge and Koelman proposed dissipative particle dynamics (DPD) as an approach to describe the hydrodynamic behavior of a fluid at a coarse-grained level with a particle-based method [19]. The study of hydrodynamic phenomena is prohibitively expensive in all-atom molecular dynamics even with high-performance computer tools because a large number of particles and long simulation times are required to properly sample Reynolds number [19,26]. Furthermore, the DPD method alleviates two drawbacks of stochastic dynamics: the nonconservation of the linear and angular momentum of the system and the loss of local hydrodynamic correlations between particles [27]. DPD is now a well-accepted method for simulating soft matter fluids. Additional details on the application of DPD to the two-chain system will be presented in Sec. II.

In this work, we apply the DPD simulation method to study the interaction between a strong polycation that remains fully charged and a weak polyanion whose charge density is being varied by the *p*H value ranging from $p\mathrm{H} = 1$ to 14, corresponding to a neutral and to a fully charged chain, respectively. Both polyelectrolytes are linear chains in aqueous solution and their respective counterions are included explicitly. For every *p*H, the structure of the complex is analyzed in terms of radial distribution functions, end-to-end distances, radii of gyration of both chains, and the radius of gyration of the complex. Our model represents a complex made by an anionic weak and a cationic strong polyelectrolyte emulating systems widely used in experimental studies. We will use our model as generic as possible and the interaction parameters in the original DPD conservative forces will remain the same for all interacting pairs (see Sec. II). This simple model is nevertheless sufficient to investigate relevant features of

the polyelectrolyte complex and to analyze physicochemical effects on the formation mechanism.

The rest of the work is organized as follows: In Sec. II, the DPD simulation technique and the electrostatic interactions between particles are described. In Sec. III, the simulations details are specified. The results and their discussion are presented in Sec. IV. The conclusions are given in Sec. V and, finally, the references.

II. SIMULATION TECHNIQUE

A. Contributions to the force between pairs of DPD particles

The DPD is a stochastic simulation technique with explicit solvent particles that allows the inclusion of hydrodynamic effects, which could not be a simple task in Monte Carlo, molecular dynamics, or Brownian dynamics simulation methods. This method has been applied in studies of microphase separation of polymer-surfactant mixtures in aqueous solutions, colloidal movement in explicit solvent, and the breaking of a flat membrane to the incorporation of nonionic surfactants. The technique was also applied to study the stability of emulsions, i.e., surfactants in a water-oil interface, characterizing its efficiency to reproduce experimental surface tensions, and recently in the study of polymeric brushes, among others [28,29].

DPD particles correspond to coarse-grained entities representing a collection of molecules or molecular groups. DPD has the advantage that it can be used for modeling physical phenomena occurring at longer time and larger spatial scales than atomistic molecular dynamics (MD), it utilizes a momentum-conserving thermostat and soft repulsive interactions between the beads. The thermostat is generated by dissipative and random forces and the equilibrium states of the system are sampled in the canonical ensemble, thermodynamically characterized by fixed number of particles, volume, and temperature. In DPD simulations, the particles interact via soft pair potentials allowing them to overlap. By grouping a set of atoms or molecules, a bead depicts a small region of fluid. The motion of the beads is governed by Newton's laws and the total force acting on them. The solvent is modeled as neutral particles while polymers are made of beads that are kept together via harmonic potentials. Depending on the system or the phenomenon under study, additional conservative forces can be included. In the systems here simulated, five contributions to the total force on a bead i, $\mathbf{F}_i$, were considered. They are

$$\mathbf{F}_i = \sum_{j\neq i}\left(\mathbf{F}_{ij}^C + \mathbf{F}_{ij}^D + \mathbf{F}_{ij}^R\right) + \sum_{j\neq i}\left(\mathbf{F}_{ij}^S + \mathbf{F}_{ij}^E\right), \qquad (1)$$

where the first sum includes the forces due to the interaction of neighboring particles and the second models the forces between bonded monomers along the polymers and the electrostatic interaction between charged beads, whether they are charged monomers or counterions. The superscripts C, D, R, S, and E mean conservative, dissipative, random, spring harmonic, and electrostatic interactions, respectively.

The conservative force is a soft repulsion term that acts along the lines of the centers and is given by $\mathbf{F}_{ij}^C = a_{ij}\omega^C(r_{ij})\hat{\mathbf{e}}$, where $r_{ij} = |\mathbf{r}_{ij}| = r$ is the distance between ith and jth particles, the unit vector $\hat{\mathbf{e}} = \mathbf{r}_{ij}/r_{ij}$, and a_{ij} is the parameter of maximum repulsion between them. This parameter can be obtained through $a_{ij} = a_{ii} + \chi_{ij}/0.306$, where χ_{ij} is the Flory-Huggins parameter. In this work, we will keep the same values for the parameters a_{ij}'s in the conservative force, allowing the electrostatics to play the main role in the complex formation. DPD includes a linear weight function $\omega(r) = 1 - r/R_c$ for $r < R_c$ and $\omega(r) = 0$ for $r > R_c$, where R_c is the cutoff distance. The weight function for the conservative force is $\omega^C(r) = \omega(r)$. The dissipative force $\mathbf{F}_{ij}^D$ providing a viscous drag to the beads is given by $\mathbf{F}_{ij}^D = -\gamma_{ij}\omega^D(r_{ij})[\hat{\mathbf{e}}_{ij}\cdot\mathbf{v}_{ij}]\hat{\mathbf{e}}_{ij}$, where γ_{ij} determines its strength, $\gamma_{ij} = \gamma_{ji} > 0$, and $\mathbf{v}_{ij} = \mathbf{v}_i - \mathbf{v}_j$ is the difference of particle velocities. Conversely, the random force $\mathbf{F}_{ij}^R$ counteracts this cooling by applying random kicks to the beads that tend to increase the relative velocities of the adjacent pairs. This force is given by $\mathbf{F}_{ij}^R = \sigma_{ij}\omega^R(r_{ij})\xi_{ij}\hat{\mathbf{e}}_{ij}$, where σ_{ij} determines the strength of the random force, ξ_{ij} is a random number which has zero mean and unit variance. The weight functions for the dissipative and random forces are related through $\omega(r) = \sqrt{\omega^D(r)} = \omega^R(r)$. The force that holds attached the monomers on the polyelectrolytes is given by $\mathbf{F}_{ij}^S = -K(r - r_0)\mathbf{r}_{ij}/r$, where K is the bond constant, chosen as in Ref. [30], in SI units $K = 4.0$ N/m and $r_0 = 0$.

Español and Warren [31] showed that the system will sample the canonical distribution if the dissipative and random forces obey the fluctuation-dissipation theorem $\gamma = \sigma^2/2k_BT$, where $\gamma = \gamma_{ij}$ and $\sigma = \sigma_{ij}$ for any i and j, T is the absolute temperature, and k_B is the Boltzmann's constant. Moreover, $\mathbf{F}_{ij}^D$ and $\mathbf{F}_{ij}^R$ act as an in-built thermostat.

In DPD the conservative force is well defined at $r = 0$, allowing full overlap between particles. However, the electrostatic energy of two point charges diverges at $r = 0$, then the addition of the electrostatic interaction of point charges could result in the formation of artificial ionic pairs [32]. In order to overcome this effect, Groot proposed the use of charge distributions instead of point charges. In this context, González-Melchor *et al.* [33] proposed to use the Ewald method in combination with charge distributions on DPD particles.

B. Electrostatic interactions in DPD systems

Here, we will use the methodology developed in [33]. To remove the divergence in $r = 0$, a Slater-type charge distribution was considered on each charged DPD particle

$$\rho(R) = \frac{q}{\pi\lambda^3}e^{-2R/\lambda}, \qquad (2)$$

where λ is the decay length of the distribution, R is the radial distance measured from the center of the particle, and q is the total charge on it.

The energy and the force between two Slater distributions, separated from center to center by a distance $r = r_{ij}$, are given by [34]

$$u_{ij}^E(r) = \frac{1}{4\pi\epsilon_0\epsilon_r}\frac{q_iq_j}{r}[1 - (1 + \beta r)e^{-2\beta r}] \qquad (3)$$

and

$$\mathbf{F}_{ij}^{E} = \frac{1}{4\pi\epsilon_0\epsilon_r}\frac{q_i q_j}{r^2}\{1 - e^{-2\beta r}[1 + 2\beta r(1+\beta r)]\}\hat{r}, \quad (4)$$

where $\beta = 1/\lambda$, and ϵ_0 and ϵ_r are the dielectric constants of vacuum and water at room temperature, respectively.

In the right-hand side of Eqs. (3) and (4), the first term in each is the long-range $1/r$ contribution. Since these contributions are not computationally practical, they are calculated using the Ewald expression [33,35] that will be given in Eq. (5), where the electrostatic interactions are decomposed into real and reciprocal space contributions which are short-ranged sums, plus a self-energy term. The remaining terms in Eqs. (3) and (4) are also taken into account with the advantage that they are short ranged, therefore, do not require any special treatment and their calculation is added directly to the conservative contributions. The total Coulomb energy for a periodic system of N point charges with positions $\mathbf{r}_1, \mathbf{r}_2, \ldots, \mathbf{r}_N \equiv \mathbf{r}^N$ is written as

$$U(\mathbf{r}^N) = \frac{1}{4\pi\epsilon_o\epsilon_r}\left[\sum_i\sum_{j>i} q_i q_j \frac{\mathrm{erfc}(\alpha r)}{r} + \frac{2\pi}{V}\sum_{\mathbf{k}\neq 0}^{\infty} Q(\mathbf{k})\, S(\mathbf{k})\, S(-\mathbf{k}) - \frac{\alpha}{\sqrt{\pi}}\sum_i^N q_i^2\right], \quad (5)$$

where q_i is the charge of particle i, $V = L^3$ is the simulation cell's volume of length L, and $\mathrm{erfc}(x)$ is the complementary error function. The terms in the right-hand side of Eq. (5) are the real, the reciprocal, and the self-energy contributions, $\mathbf{k}$ is the reciprocal vector $\mathbf{k} = 2\pi(m_x, m_y, m_z)/L$, where m_x, m_y, m_z are integer numbers. The parameter α controls the contribution of the Coulomb interactions in real space. The quantities $Q(\mathbf{k})$ and $S(\mathbf{k})$ are defined as

$$Q(\mathbf{k}) = \frac{e^{-k^2/4\alpha^2}}{k^2} \qquad S(\mathbf{k}) = \sum_{i=1}^{N} q_i\, e^{i\mathbf{k}\cdot\mathbf{r}}, \quad (6)$$

where k is the magnitude of the reciprocal vector $\mathbf{k}$.

For the system made of particles carrying a charge distribution on each bead, Eq. (5) is used in the calculation of the first term in Eq. (3) and the corresponding Ewald force is used to evaluate the $1/r^2$ term in Eq. (4). In this way, we calculated these terms as is commonly done in atomistic simulations, keeping in mind that in the DPD description, they are just part of the electrostatic contribution. The full electrostatic pair potential and the electrostatic force are then given by Eqs. (3) and (4), respectively, and their evaluation makes use of the Ewald summation method. Since the electrostatic force is conservative, the sum of the $\mathbf{F}_{ij}^{E}$ contained in Eq. (4) and the original conservative part $\mathbf{F}_{ij}^{C}$ in Eq. (1) will determine the thermodynamic behavior of the system.

III. SIMULATION DETAILS

We considered two polyelectrolyte chains of opposite charge made of 100 monomers each in aqueous solution. In this study, the polycation is fully charged whereas the charge of the polyanion was varied. The charge fraction on the chains $\phi+$ and $\phi-$ are given by $\phi\pm = N^{\pm}/N^{t}$, where N^{+} and N^{-} are the number of positively and negatively charged beads, respectively, and $N^{t} = 100$ is the total number of beads in each polyelectrolyte. Here, the polycation is kept fully charged so its charge fraction is always 1 while for the polyanion the charge fraction was varied, taking values $\phi- =$ 0 (neutral polymer), 0.1, 0.2, 0.25, 0.34, 0.5, 0.66, 0.8, and 1.0 (polyanion fully charged). For simplicity, the polyanion charge fraction will be denoted as ϕ hereafter. To warrant charge neutrality, 100 counterions of net charge $-e$ concerning to the polycation, and the necessary counterions with net charge $+e$ corresponding to the polyanion, were introduced in the systems. For each charge fraction, the charged monomers were distributed as uniformly as possible along the polyanion.

The simulations were done in the canonical (NVT) ensemble, i.e., at constant number of particles, volume, and temperature. Periodic boundary conditions were applied in the three directions. The total particles were randomly placed in a cubic box of reduced volume $V = L^3$, with the side $L = 25R_c$ being R_c the cutoff radius. In the simulations we use the cutoff radius, the bead mass, and the thermal energy as the reference units to measure any other quantity. The temperature was kept at 298 K for all the simulations and the total number of DPD particles was 46 875 in each case. The interaction parameters between beads for the conservative, dissipative, and random forces were $a_{ij} = 78.33$ for all pairs ij, which reproduce the compressibility of pure water at room temperature [36]; $\gamma_{ij} =$ 4.5 and $\sigma_{ij} = 3.0$ for all i, j, these values lead to a reduced temperature $T^* = T/T_0 = 1$ with $T_0 = 298$ K. The value R_c is obtained using the relationship $R_c = (\rho^* N_m V_m/N_A)^{1/3}$, where ρ^* is the reduced density of DPD particles, N_m is the number of real water molecules modeled into one DPD particle, $V_m =$ 18 $\mathrm{cm^3\,mol^{-1}}$ is the molar volume of water, and N_A is the Avogadro's number and the total reduced density is equal to 3. Then, $R_c = 4.48N_m^{1/3}$ Å. Using $N_m = 3$, gives $R_c = 6.4633$ Å [33]. The parameter that controls the contribution in the real space is $\alpha = 0.15$ $\mathrm{Å^{-1}}$. Regarding the reciprocal part, we calculated the summation using a maximum number of vectors defined by $(m_x, m_y, m_z)^{\max} = (5, 5, 5)$. The parameter of the Slater distribution assigned on charged particles was $\beta^* = \beta R_c = R_c/\lambda = 0.929$ [33]. Each simulation was conducted with 1×10^5 steps for equilibration and additional 2×10^6 for calculating average properties.

IV. RESULTS AND DISCUSSION

In this section, we discuss the simulation results obtained for the polyanion-polication system in water when the polyanion charge fraction changes with the *p*H through the so-called cooperativity parameter q, and a modified Hendersson-Hasselbach equation, both described by Petrov *et al.* in experimental measurements [22]. In order to analyze the effect of *p*H on the charge fraction of the polyanion, the polycation is maintained fully charged in all the simulations over all the *p*H range, we have used an analysis similar to that made by González-Melchor *et al.* [33], where the charge fraction of the weak anionic polyelectrolyte changes due to the *p*H value

TABLE I. Average values of the end-to-end distance $\langle R^*_{ee}\rangle$ and radius of gyration $\langle R^*_g\rangle$ of the polycation and the polyanion, and radius of gyration of the complex $\langle R^*_g\rangle_{\text{complex}}$ at different charge fraction ϕ and pH.

ϕ	0	0.1	0.2	0.25	0.34	0.5	0.66	0.8	1.0
pH	1	4.9	5.1	5.2	5.3	5.5	5.6	5.8	14
$\langle R^*_{ee}\rangle poly+$	22.6469	20.6930	17.7957	17.8648	17.0943	13.6521	8.2254	4.8252	3.8931
$\langle R^*_{ee}\rangle poly\phi$	8.5494	7.0046	8.7891	11.4381	12.7806	11.7234	6.4450	4.0408	4.2451
$\langle R^*_g\rangle poly+$	7.8215	7.3543	6.5499	6.4265	6.1315	5.1615	3.5244	2.5705	2.1760
$\langle R^*_g\rangle poly\phi$	3.6458	3.1794	3.8080	4.5735	4.9740	4.6218	3.1316	2.3028	2.1767
$\langle R^*_g\rangle_{\text{complex}}$		10.4006	9.2630	9.0885	8.6713	7.2995	4.9843	3.6353	3.0773

according to

$$p\text{H} = n\,\log_{10}\left(\frac{\phi}{1-\phi}\right) + p\text{Ka}, \tag{7}$$

where pKa is the acidity constant chosen to be 5.5 which is a typical value of a weak polyelectrolyte. Petrov *et al.* [22] observed that the PAH and the PSS do not fit the classical Hendersson-Hasselbach equation [Eq. (7), with $n = 1$], as in the case of a monobasic acid relative to proton binding. Here is important the introduction of the so-called cooperativity parameter q, which is a measure of the free energy of interaction between neighbor proton-accepting sites $\Delta G = -R\,T\,\ln(q)$, where $q < 1$, $q = 1$, and $q > 1$ are the q values for anticooperative, noncooperative, and cooperative processes, respectively. In this context, Ising methods are very useful to describe short-range interactions [22,37] which can affect the q value. The empirical parameter n in the extended Henderson-Hasselbach equation [Eq. (7)] could be related with the parameter q from the Ising model through $q = n^{-2}$, as Katchalsky and Sputnik [38] and Leyte and Mandel [39] have described in the titration behavior of a polyelectrolyte. In order to apply our results to a realistic system we have chosen $q = 3.06$, which corresponds to a complex formed by PSS and PAH in water according to Petrov *et al.* [22]. On the other hand, long-range electrostatic interactions could also affect the value of q. Some MD or Monte Carlo studies take into account this type of interaction by using the Debye-Hückel potential, where counterions are not explicitly included [40]. In DPD, where the particles represent fluid regions, the long-range electrostatic interactions are taken into account via the potential between charged beads [Eq. (3)], where the first term on the right-hand side represents the interaction between point charges whereas the second one could be thought of as related to screening effects.

Equation (7) was obtained by considering that initially the polyanion is uncharged at very low pH. As OH^- ions are added, the polyelectrolyte starts to deprotonate, increasing the anionic charge of the polyelectrolyte chain until reaching an equilibrium where there is a balance of dissociated species (polyanion-counterion). In this model, the polyanion contains two different groups: one of these is neutral and the other one behaves as a monoprotic acid. Our molecule is mapped into 100 DPD beads, similar to that shown in Fig. 7 in Ref. [33]. So, when the value of pH is varying, the charge of the polyanion is changing between 0 and 1 where pH is 1 and 14, respectively (see Table I). Both polyelectrolytes are contained in a simulation cell with water DPD particles and their respective counterions. Figure 1 shows snapshots of four cases in equilibrium configurations. The green beads correspond to the fully charged polycation, and the red and pink spheres represent negatively charged and uncharged beads on the polyanion. Figure 1(a) represents the case at pH = 1 where we have a completely protonated polyanion (uncharged). Both chains are separated from one another. Figure 1(b) shows the case at pH = 4.9 with a polyanion charge fraction of 0.1. The snapshot shows that the polyanion folds into a section of the polycation. However, the polycation remains mostly unfolded during the complex process in the simulation. In Fig. 1(c), the pH is increased until 5.5 ($\phi = 0.5$), the two polyelectrolyte chains are folded resulting in an extended polyelectrolyte complex and, finally, Fig. 1(d) shows a solution situation at pH = 14, where both polyelectrolytes are fully charged, and the chains fold completely to form a compact polyelectrolyte complex. These results show a similar behavior as recent investigations with other systems, for example, Jiang *et al.* [4] studied the assembly of micellar nanoparticles with

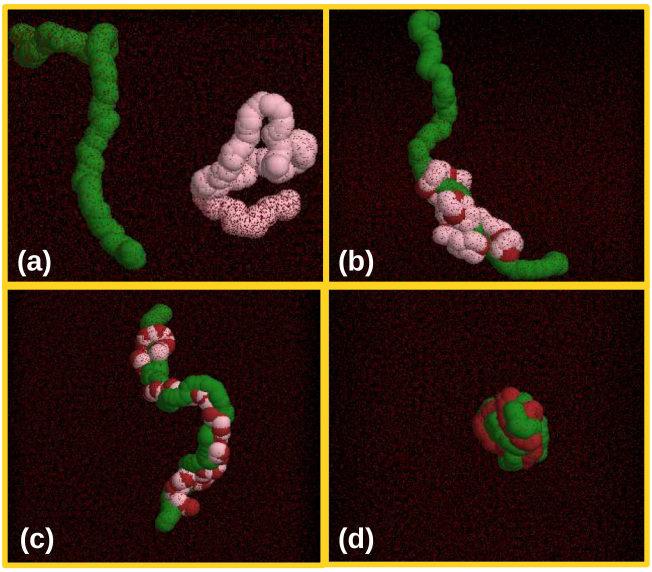

FIG. 1. Systems at equilibrium conditions. Fully charged cationic polyelectrolyte interacting with a polymer of different charge fractions: (a) polyanion fully protonated; (b) polyanion of charge fraction $\phi = 0.1$ (pH = 4.9); (c) polyanion of charge fraction $\phi = 0.5$ (pH = 5.5); and (d) polyanion of charge fraction $\phi = 1$ (pH = 14). Green color is assigned for the polycation, pink for the neutral beads, and red for the negatively charged beads. Water molecules and counterions are omitted for clarity.

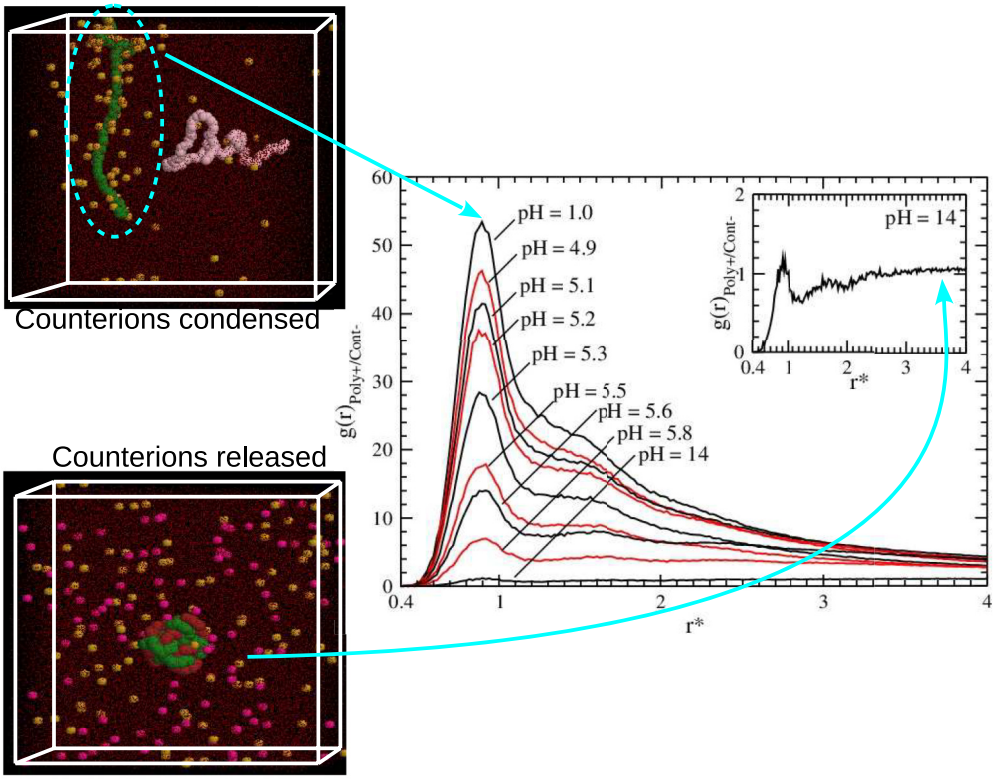

FIG. 2. Pair correlation function between the polycation and its negative counterion $g(r)_{poly^+/cont^-}$ as a function of the pH and the charge fraction ϕ, indicated in each curve in the figure. The inset shows the correlation at $p\mathrm{H} = 14$. Two snapshots taken from the simulations are also shown. The upper snapshot on the left represents the case at $p\mathrm{H} = 1$, where the polycation (green chain) and its counterions (in yellow) are interacting with the fully protonated polyanion behaving as a neutral polymer (pink). Here, the counterions are close to the polycation (usually called condensed counterions). The lower snapshot represents the extreme case at $p\mathrm{H} = 14$, where the fully deprotonated polyanion is shown in red and their counterions in magenta; at these conditions the counterions are released allowing the formation of the compact complex.

different shapes by condensing DNA with PEG-PPA block copolymer in solvents with different polarities. The solvent polarity dictates the interactions between solvent and DNA and with polycation and PEG blocks, which in turn influence the condensation state of the complex core, i.e., their findings showed a conformational change from an extended complex in a good solvent to a very condensed compact complex in a bad solvent. In our research, the driving force for the polyelectrolyte complex formation is dictated by the release of the counterions, which is supported by the behavior of the radial distribution functions, as will be seen below. It can also be interpreted in terms of an increase in the entropy of the released counterions, just as we had discussed in a previous article [18].

A. Radial distribution functions

For a structural analysis of the particles in the system the radial distribution functions $g_{ab}(r)$ were obtained from the simulations. Since $g_{ab}(r)$ measures the probability of finding a particle of species b separated at a distance r from particle of species a, it is calculated as $g_{ab}(r) = N_{ab}(r, r + dr)/\{4\pi\rho_b[(r + dr)^3 - r^3]/3\}$, i.e., the number of particles of type b, N_{ab} in the volume defined by the spheres of radii r and $r + dr$ is divided by the volume of the shell and normalized by the bulk number density of particles b, ρ_b.

Figure 2 shows the polycation-counterion pair distribution functions $g(r)_{poly+/cont-}$, at different charge fractions. Naturally, the highest peak located at distance $r^* = 0.9$ is found at $p\mathrm{H} = 1$ ($\phi = 0$) since the polycation does not interact with the neutral polymer, its negatively charged counterions are very close around it due to their attractive electrostatic interactions. This situation is shown in the snapshot inserted up on the left in Fig. 2. This behavior is opposed to that found in the case of the polycation-counterion pair at $p\mathrm{H} = 14$. Nonetheless, the $g(r)_{poly+/cont-}$ function decreases as the charge fraction of the polyanion increases, indicating that the attraction between the polycation and the polyanion becomes more favorable given rise to the release of counterions, so that the interaction of the polycation-counterion pair weakens. The inset in Fig. 2 shows the case at $p\mathrm{H} = 14$ when the polyanion is totally charged ($\phi = 1$). Here, a small peak is observed, which is related to the high peak displayed in Fig. 4 at this same pH, indicating a strong interaction between both polyelectrolytes and a release of their counterions, leading thus to the formation of a compact complex. The snapshot corresponding to $p\mathrm{H} = 14$ ($\phi = 1$), shown below to the left in Fig. 2, evidences this fact. Studies based on MD simulations have shown similar results [10,41].

Figure 3 shows the correlation function between the polyanion (labeled as $poly\phi$) and its counterion $g(r)_{poly\phi/cont+}$, at $p\mathrm{H} = 5.5$ ($\phi = 0.5$), $p\mathrm{H} = 5.8$ ($\phi = 0.8$), and $p\mathrm{H} = 14$

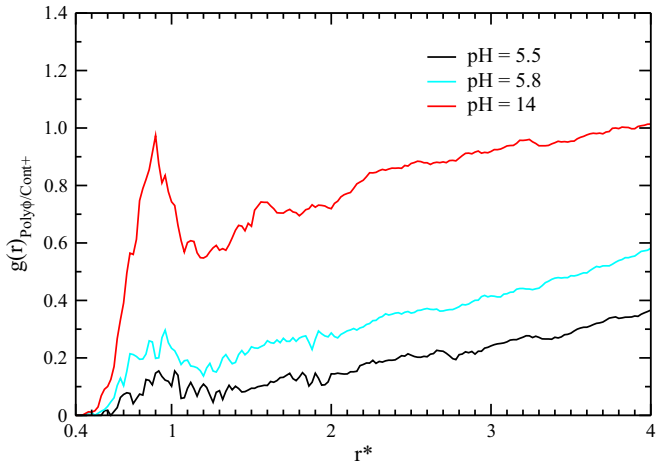

FIG. 3. Pair correlation function between the polyanion and its positive counterion $g(r)_{poly\phi/cont^+}$ as a function of the pH and the charge fraction ϕ for values $\phi = 0.5$, 0.8, and 1.

($\phi = 1$). A peak is observed at $r^* = 0.9$. From all the studied cases, the peak of lowest magnitude corresponds to $p\text{H} = 4.9$ and $\phi = 0.1$ (not shown in the figure). As ϕ increases, this peak becomes more pronounced. So, from the cases shown in Fig. 3 the pair correlation at $p\text{H} = 5.5$ has a low intensity whereas at $p\text{H} = 14$ it has the highest magnitude. Nevertheless, the intensity of this radial distribution function is considerably lower than those of other pairs (see Figs. 2 and 4). This is due to the fact that for low pH, the polyanion has a low amount of negative charges and therefore low number of counterions. Consequently, a peak of low magnitude is achieved. We have observed an opposite effect of the $g(r)_{poly^+/cont^-}$ with respect to the $g(r)_{poly\phi/cont^+}$, the peak for the former decreased while the peak for the latter increased when the pH was increased. In fact, we really expect an increase in the correlation of pairs polyanion-counterion which is due to an increase in the ϕ on the anionic polyelectrolyte in a basic solution. On the other hand, considering the

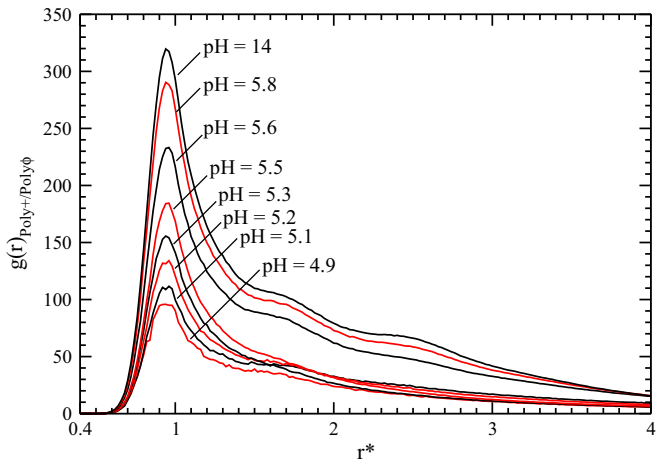

FIG. 4. Pair correlation function between the polycation and the polyanion $g(r)_{poly^+/poly\phi}$ as a function of the charge fraction. The numbers signaling the curves correspond to pH and ϕ values.

case of $p\text{H} = 5.5$, when we compared the magnitude of the peaks from Figs. 2 and 3, we observed that the correlation polycation-counterion is higher than that of the polyanion-counterion until reaching the same peak magnitude at $p\text{H} = 14$ (fully charged polyelectrolytes) where we have an equal number of dissociated ions in the whole system, therefore, we should expect a same interaction of the charged chain and its counterions for both polyelectrolytes. Indeed, a systematic study on the different conformations adopted by the chains needs to be performed during complex formation; in this context, Trejo-Ramos *et al.* [42] have shown that the interaction between oppositely charged polyelectrolytes produces large aggregates where the external part of the complex exhibits a larger population of positive monomers when the chains are asymmetric in size. Marquez *et al.* [17] suggested the structure of the polyelectrolyte complex. In the core, polyelectrolyte chains of opposed charge neutralize each other. In the shell, an excess of polycation gives the complex a positive charge (chains more exposed to the medium). Those findings support the idea that there is greater correlation between the polycation and the polyanion in the complex formation. The correlation between both polyelectrolyte chains, quantified through $g(r)_{poly+/poly\phi}$, is shown in Fig. 4 as function of the charge fraction, except for $p\text{H} = 1$ ($\phi = 0$) which corresponds to the case where we do not see the formation of a complex. In all cases, a pronounced peak is observed at $r^* = 0.9$. The peak of lowest intensity corresponds to $p\text{H} = 4.9$, then it increases as pH is higher such that at $p\text{H} = 14$ it has the highest intensity. This effect is due to the greater number of negative charged monomers on the polymer as pH increases, showing that the attractive interaction between the two chains is more cooperative. This fact leads to the conclusion that the polycation is structurally more affected when the polyanion is fully charged as compared to a polycation interacting with a polymer of low negative charge fraction. The obtained results of Figs. 2 and 4 are in good agreement with earlier simulation predictions [18], demonstrating that the driving force for the overall complexation process is determined by both the attractive electrostatic interactions (related to Fig. 4), and also by the process of low-molecular weight counterion release (related to Fig. 2), which is in agreement with the explanation that an increase in the entropy of the counterion strongly leads the complexation process.

B. Polyelectrolyte complexation: Radius of gyration and end-to-end distance

A polyelectrolyte chain differs considerably from its neutral analog because of its highly charged backbone and long-ranged nature of electrostatic interaction with charged species. The size and shape of a polyelectrolyte complex depend on the strength of electrostatic interaction between polyelectrolytes of opposed charge. The polyelectrolyte chains can adopt a great number of conformations depending on the medium and this effect may have repercussions in the form of the final complex. The distance between the first and the last link, called the end-to-end distance R_{ee}, and the radius of gyration R_g are useful parameters for characterizing representative polyelectrolyte extension. To quantify the effect of varying the charge fraction of the polyanion on the polycation, R_{ee} and

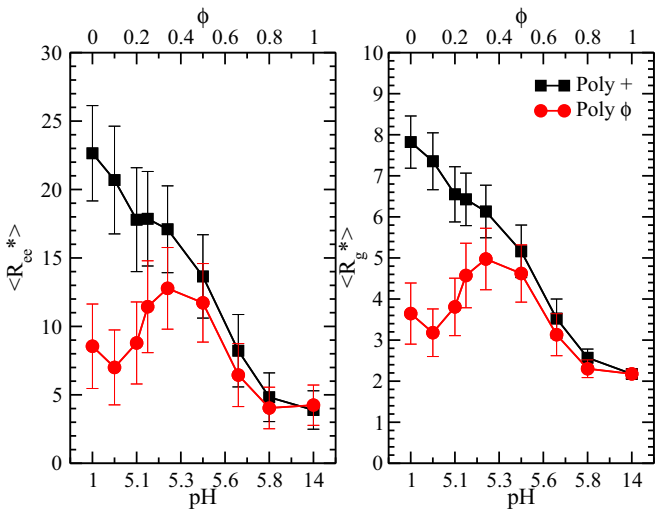

FIG. 5. On the left, end-to-end distance $\langle R^*_{ee} \rangle$ for the polycation and the polyanion. On the right, radius of gyration $\langle R^*_g \rangle$ for the polycation and the polyanion. Both properties as functions of the *p*H. The error bars are shown.

R_g of each polyelectrolyte were computed using the unfolded positions of the monomers and evaluating the time averages of the squared quantities $\langle R^2_{ee} \rangle$ and $\langle R^2_g \rangle$, where $R^2_{ee} = (\mathbf{r}_m - \mathbf{r}_1)^2$, being m and 1 the last and the first monomer of the chain. Assuming equal mass particles, the squared radius of gyration is calculated as $R^2_g = 1/(N_m) \sum_{i=1}^{N_m} (\mathbf{r}_i - \mathbf{R}_{\text{c.m.}})^2$, where N_m is the number of monomers, $\mathbf{r}_i$ is the position of the ith monomer, and $\mathbf{R}_{\text{c.m.}} = 1/(N_m) \sum_{i=1}^{N_m} \mathbf{r}_i$ is the center of mass of the chain.

On the left of Fig. 5, the variation of the end-to-end distance for both polyelectrolytes is shown for different charge fractions. We observed that for *p*H = 1 the greatest magnitude of $\langle R^*_{ee} \rangle$ is achieved for the polycation while for the neutral polymer an intermediate end-to-end distance is obtained. In general, as the *p*H increases, the end-to-end distance of the polycation decreases, taking the lowest value when *p*H = 14. On the other hand, the $\langle R^*_{ee} \rangle$ distance of the polyanion decreases slightly when the charge fraction goes from the neutral case to *p*H = 4.9, then for *p*H from 4.9 to 5.2 it increases reaching a maximum after which $\langle R^*_{ee} \rangle$ abruptly decreases in the range from *p*H = 5.2 to 5.8. Thereafter, the decreasing of $\langle R^*_{ee} \rangle$ from *p*H = 5.8 to 14 is minimal. On the right of Fig. 5, the radius of gyration for both polyelectrolyte chains is shown as function of the charge fraction. In this figure, the radius of gyration exhibits a similar behavior as that obtained for $\langle R^*_{ee} \rangle$: the highest magnitude of radius of gyration for the polycation is obtained for *p*H = 1 and then subsequently decreases as the charge fraction increases whereas the radius of gyration of the neutral polymer initially has an intermediate value, decreasing as *p*H goes from 1 to 4.9. Then, an increase in $\langle R^*_g \rangle$ occurs achieving a maximum at *p*H = 5.2 and then it decreases as *p*H grows from 5.2 to 5.8. From then on, the radius of gyration of the polyanion tends to a limit value. Recently, Goswami *et al.* [43] used MD simulations to study systems formed by a polycation chain interacting with anionic surfactants and obtained similar results. They modified the number of charged monomers on the polyelectrolyte chain and found that the radius of gyration and the end-to-end distance showed a similar dependence with the number of charges on the chain except at low number of charges. The fact that $\langle R^*_{ee} \rangle$ and $\langle R^*_g \rangle$ increase for the polyanion in the range $4.9 < p\text{H} < 5.2$ is due to electrostatic interaction between the charged monomers that results in a chain swelling. Conversely, the polycation $\langle R^*_{ee} \rangle$ and $\langle R^*_g \rangle$ decrease for all *p*H. This decrease suggests that the electrostatic interaction between the polyelectrolytes is getting stronger. Thus, the average size of the polyanion, measured through $\langle R^*_{ee} \rangle$ and $\langle R^*_g \rangle$, decreases for *p*H >5.2, leading to the formation of a compact complex.

C. Radius of gyration of the complex

In a previous work [18], we estimated the radius of gyration of a two-chain polyelectrolyte complex from the radius of gyration of the individual chains. This approach was based on the results obtained by Meng *et al.* [44], who related the hydrodynamic radius of one polymer chain in solution with its radius of gyration. In order to find a theoretical equation for the radius of gyration of a polyelectrolyte complex contained in an aqueous solution, we have proposed the Fox-Flory model as a first approach in a dilute solution; this is the case of our system. We have justified this description due that the net charge of the polyelectrolyte complex is decreasing when the charge fraction of the polyanion is increasing, until reaching a zero charge, i.e., when the polyanion charge fraction is equal to 1. Therefore, the Fox-Flory theory can be thought as useful to describe the polyelectrolyte complex conformation, like in other polyelectrolyte systems with moderate salt concentration or weak polyelectrolyte situations [45]. The Fox-Flory [46] relation to obtain the radius of gyration of the complex, once the complex has been formed, is $\langle R^*_g \rangle_{\text{complex}} = \frac{M_{\text{complex}}[\eta]_{\text{complex}}}{\vartheta_{\text{complex}}}$, where M_{complex} is the molecular weight of the polymer complex, $[\eta]_{\text{complex}}$ is the intrinsic viscosity, and $\vartheta_{\text{complex}}$ is a Flory's parameter associated with the complex-solvent interaction. Moreover, the intrinsic viscosity is related with the Mark-Houwink equation [44] that sets $[\eta] = k_{\text{complex}} M^a_{\text{complex}}$, where k_{complex} and a are the Mark-Houwink parameters, which depend on the specific polymer, the solvent, and the temperature [44]. Given that both polyelectrolyte chains have the same size, the chains have equal masses, that is, $M^+ = M^\phi$, where M^+ and M^ϕ are the molecular weights of the polycation and the polyanion with variable charge fraction, respectively. Then, the total mass of the complex is $M_{\text{complex}} = M^+ + M^\phi = 2M^+$. Thus, the radius of gyration of the complex is written as

$$R^3_{g\text{-complex}} = \frac{M^+[\eta_{\text{complex}}]}{\vartheta^{\text{complex}}} + \frac{M^\phi[\eta_{\text{complex}}]}{\vartheta^{\text{complex}}}. \tag{8}$$

This equation includes information of both polyelectrolyte chains. So, the intrinsic viscosity can be rewritten as $[\eta_{\text{complex}}] = k_{\text{complex}} M^a_{\text{complex}} = k_{\text{complex}} (2M^+)^a$. Combining the Mark-Houwink relation with Eq. (8) we obtain

$$R^3_{g\text{-complex}} = \frac{k_{\text{complex}} \vartheta^+}{k^+ \vartheta_{\text{complex}}} (2)^{3/2} R^3_{g+}, \tag{9}$$

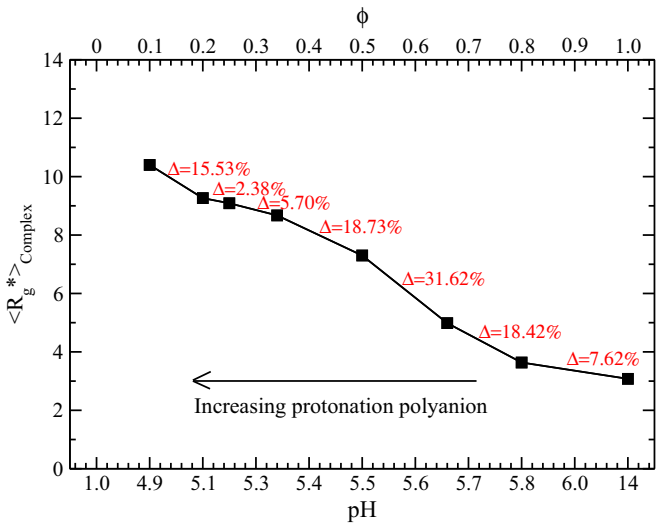

FIG. 6. Radius of gyration of the complex as a function of the charge fraction ϕ and as a function of the pH. The Δ values indicate the percentage of change of the complex radius of gyration in relation to the initial case ($\phi = 0.1$, $p\text{H} = 4.9$) and the last case ($\phi = 1$, $p\text{H} = 14$) values.

where R_g^+ and ϑ^+ are the radius of gyration and the Flory's parameter of the polycation, respectively, and we have taken $a = \frac{1}{2}$ and considered the fact that both polymers have the same size. In [18] the assumptions $\vartheta_{\text{complex}} \approx \vartheta^+$ and $k_{\text{complex}} \approx k^+$ were made by considering that the polycation and the complex have approximately the same solvent interaction under very diluted conditions. With these considerations we obtain

$$R_{g\text{-complex}} = 2^{1/2} R_g^+. \tag{10}$$

The results for the radius of gyration of the complex, obtained using Eq. (10), are shown in Fig. 6. In it, we observed the change of the radius of gyration of the complex as function of the charge fraction. To have information about the change in the size of the polyelectrolyte complex at different pH values, we calculated a delta factor Δ. This factor is defined in percentage as

$$\Delta = \left[1 - \frac{[\Delta_T] - [\Delta_i]}{[\Delta_T]}\right] \times 100\%, \tag{11}$$

where $\Delta_T = \langle R_g^* \rangle_{\text{complex},\phi=0.1} - \langle R_g^* \rangle_{\text{complex},\phi=1}$ measures the difference between the radius of gyration of the complex, obtained for the lowest charge fraction $\phi = 0.1$ where $\langle R_g^* \rangle_{\text{complex}} = 10.4$ and that obtained for the highest charge fraction $\phi = 1$ where $\langle R_g^* \rangle_{\text{complex}} = 3.07$, whereas Δ_i measures the difference in the radius of gyration of the complex obtained for two consecutive charge fraction values i and $i+1$, given by $\Delta_i = \langle R_g^* \rangle_{\text{complex},\phi_i} - \langle R_g^* \rangle_{\text{complex},\phi_{i+1}}$. The Δ values are also included in Fig. 6. The calculated end-to-end distance and the radius of gyration of the individual polymeric chains, obtained directly from the simulations, and the radius of gyration of the complex, obtained through Eq. (10), are given in Table I.

According to the values of Δ (displayed on Fig. 6), from $p\text{H} = 4.9$ to 5.1, the Δ is 15.53% but from $p\text{H} = 5.1$ to 5.3, Δ decreases considerably to a smaller value of about 5.7. The Δ's associated with great changes occur from $p\text{H} = 5.5$ to 5.8, where the polyelectrolyte complex changed from an extended to a compact shape. In this way, at $p\text{H} = 14$ a globular complex is obtained, as observed in the snapshot in Fig. 1(d).

V. CONCLUSIONS

The formation of a complex of two symmetrical polyelectrolyte chains of opposite charge, in which the charge fraction of the negative polyelectrolyte is varied due to the increasing of pH, was studied by dissipative particle dynamics simulations. The radial distribution function results show that for solutions at $p\text{H} < p\text{Ka}$, i.e., for low charge fractions on the polyanion ($\phi = 0$–0.35), the counterions of negative charge are very localized along the positively charged polyelectrolyte and a weak correlation between the charged chains was found, producing an extended polyelectrolyte complex. When the pH increases above the pKa, we found that the probability of finding together the positively charged polymer with the negatively charged polyelectrolyte increased and the counterions are less localized than in the case at $p\text{H} < p\text{Ka}$, leading to the formation of a compact polyelectrolyte complex. The transition of passing from an extended to a compact complex is originated from both the decrease in the protonation of the polyanion and the increasing release of counterions. The radius of gyration of the polycation decreased monotonically with the pH, while the radius of gyration of the polyanion increased up to a maximum at $p\text{H} \sim p\text{Ka}$ and eventually decreased when the $p\text{H} > p\text{Ka}$. Moreover, the radius of gyration of the complex showed a smooth decrease in size when the charge fraction of the polyanion increased through the pH, however, when the decreasing factor in the size of the complex was evaluated [see Eq. (11) and Fig. 6], the highest step of around 32% was found between $\phi = 0.5$–0.6, i.e., at $p\text{H} \sim p\text{Ka}$. This finding suggests that the transition from an extended to a compact complex starts at around the dissociation acid constant of the weak polyelectrolyte. In a previous work, the transition from an extended to a compact complex was observed changing the size of the anionic chain and the concentration of salt in the solution as the mechanism of formation. The particular case of $p\text{H} = 14$ corresponds to the case of equal size chains without salt, studied in [18] [see Figs. 6(a) and 6(c) with percentage length ratio $\delta = 100$]. Finally, we have shown that changing the protonation degree of one of the chains through the pH can also serve as a mechanism for tuning the complex from rodlike to globular shape.

ACKNOWLEDGMENTS

This work was supported by Programa para el Desarrollo Profesional Docente (SEP-Mexico) and by the CA Física Computacional de la Materia Condensada. The authors thankfully acknowledge the computer resources, technical expertise, and support provided by the Laboratorio Nacional de Supercómputo del Sureste de México, CONACYT network of national laboratories.

[1] E. Raphael and J. F. Joanny, Annealed and quenched polyelectrolytes, Europhys. Lett. **13**, 623 (1990).

[2] J. A. Marsh and S. A. Teichmann, Structure, dynamics, assembly, and evolution of protein complexes, Annu. Rev. Biochem. **84**, 551 (2015).

[3] R. S. Dias, A. A. C. C. Pais, M. G. Miguel, and B. Lindman, Modeling of DNA compaction by polycations, J. Chem. Phys. **119**, 8150 (2003).

[4] X. Jiang, W. Qu, D. Pan, Y. Ren, J. M. Williford, H. Cui, E. Luijten, and H. Q. Mao, Plasmid-templated shape control of condensed DNA-block copolymer nanoparticles, Adv. Mater. **25**, 227 (2013).

[5] L. C. Gosule and J. A. Schellman, Compact form of DNA induced by spermidine, Nature (London) **259**, 333 (1976).

[6] D. Porschke, Dynamics of DNA condensation, Biochemistry **23**, 4821 (1984).

[7] E. Raspaud, M. O. Cruz, J. L. Shikorav, and F. Livolant, Precipitation of DNA by polyamines: A polyelectrolyte behavior, Biophys. J. **74**, 381 (1998).

[8] V. Kabanov, Polyelectrolyte complexes in solution and in bulk, Russ. Chem. Rev. **74**, 3 (2005).

[9] V. S. Meka, M. K. G. Sing, M. R. Pichika, S. R. Nail, V. R. M. Kolapalli, and P. Kesharwani, A comprehensive review on polyelectrolyte complexes, Drug Discov. Today **22**, 1697 (2017).

[10] C. E. Sing, Development of the modern theory of polymeric complex coacervation, Adv. Colloid Interface Sci. **239**, 2 (2017).

[11] D. V. Pergushov, A. H. E. Muller, and F. H. Schacher, Micellar interpolyelectrolyte complexes, Chem. Soc. Rev. **41**, 6888 (2012).

[12] C. F. Narambuena, E. P. M. Leiva, M. Chávez-Páez, and E. Pérez, Effect of chain stiffness on the morphology of polyelectrolyte complexes. A Monte Carlo simulation study, Polymer **51**, 3293 (2010).

[13] H. Dautzenberg, Polyelectrolyte complex formation in highly aggregating systems. 1. Effect of salt: Polyelectrolyte complex formation in the presence of NaCl, Macromolecules **30**, 7810 (1997).

[14] V. Mengarelli, L. Auvray, and M. Zeghal, Phase behavior and structure of stable complexes of oppositely charged polyelectrolytes, Europhys. Lett. **85**, 58001 (2009).

[15] V. Bloomfield, DNA condensation by multivalent cations, Biopolymers **44**, 269 (1998).

[16] A. F. Thünemann, M. Müller, H. Dautzenberg, J. F. Joanny, and H. Löwen, in *Polyelectrolytes with Defined Molecular Architecture II*, edited by M. Schmidt, Advances in Polymer Science Vol. 166 (Springer, Berlin, 2004).

[17] C. Márquez-Betrán, L. Castañeda, M. Enciso-Aguilar, G. Paredes-Quijada, H. Acuñ-Campa, A. Maldonado-Arce, and J. F. Arguillier, Structure and mechanism formation of polyelectrolyte complex obtained from PSS/PAH system: Effect of molar mixing ratio, base-acid conditions, and ionic strength, Colloid Polym. Sci. **291**, 683 (2013).

[18] E. Meneses-Juárez, C. Márquez-Beltrán, J. F. Rivas-Silva, U. Pal, and M. González-Melchor, The structure and interaction mechanism of a polyelectrolyte complex: A dissipative particle dynamics study, Soft Matter **11**, 5889 (2015).

[19] P. J. Hoogerbrugge and J. M. V. A. Koelman, Simulating microscopic hydrodynamic phenomena with dissipative particle dynamics, Europhys. Lett. **19**, 155 (1992).

[20] T. Ehtezazi, U. Rungsardthong, and S. Stolnik, Thermodynamic analysis of polycation-DNA interaction applying titration microcalorimetry, Langmuir **19**, 9387 (2003).

[21] Z. Ou and M. Muthukumar, Langevin dynamics of semiflexible polyelectrolytes: Rod-toroid-globule-coil structures and counterion distribution, J. Chem. Phys. **123**, 074905 (2005).

[22] A. I. Petrov, A. A. Antipov, and G. B. Sukhorukov, Base-acid equilibria in polyelectrolyte systems: From weak polyelectrolytes to interpolyelectrolyte complexes and multilayered polyelectrolyte shells, Macromolecules **36**, 10079 (2003).

[23] D. Diddens, J. Baschnagel, and A. Johner, Microscopic structure of compacted polyelectrolyte complexes: Insights from molecular dynamics simulations, ACS Macro Lett. **8**, 123 (2019).

[24] J. Jung, W. Nishima, M. Daniels, G. Bascom, C. Kobayashi, A. Adedoyin, M. Wall, A. Lappala, D. Phillips, W. Fischer *et al.*, Scaling molecular dynamics beyond 1 00 000 processor cores for large-scale biophysical simulations, J. Comput. Chem. **40**, 1919 (2019).

[25] M. Vögele, C. Holm, and J. Smiatek, Coarse-grained simulations of polyelectrolyte complexes: MARTINI models for poly(styrene sulfonate) and poly(diallyldimethylammonium), J. Chem. Phys. **143**, 243151 (2015).

[26] T. Murtola, A. Bunker, I. Vattulainen, M. Deserno, and M. Karttunen, Multiscale modeling of emergent materials: Biological and soft matter, Phys. Chem. Chem. Phys. **11**, 1869 (2009).

[27] P. H. Hünenberger, Thermostat algorithms for molecular dynamics simulations, Adv. Polym. Sci. **173**, 105 (2005).

[28] S. Pal and C. Seidel, Dissipative particle dynamics simulations of polymer brushes: comparison with molecular dynamics Simulations, Macromol. Theory Simul. **15**, 668 (2006).

[29] J. Cheng, A. Vishnyakov, and A. V. Neimark, Morphological transformations in polymer brushes in binary mixtures: DPD Study, Langmuir **30**, 12932 (2014).

[30] R. D. Groot, Mesoscopic simulation of polymer-surfactant aggregation, Langmuir **16**, 7493 (2000).

[31] P. Español and P. B. Warren, Statistical mechanics of dissipative particle dynamics, Europhys. Lett. **30**, 191 (1995).

[32] R. D. Groot, Electrostatic interactions in dissipative particle dynamics-simulation of polyelectrolytes and anionic surfactants, J. Chem. Phys. **118**, 11265 (2003).

[33] M. González-Melchor, E. Mayoral, E. Velázquez, and J. Alejandre, Electrostatic interactions in dissipative particle dynamics using the Ewald sums, J. Chem. Phys. **125**, 224107 (2006).

[34] M. Carrillo-Tripp, Selectividad iónica de canales biológicos, Ph.D. thesis, Universidad Autónoma del Estado de Morelos, Mexico, 2005.

[35] P. P. Ewald, The calculation of optical and electrostatic grid potential, Ann. Phys. **64**, 253 (1921).

[36] R. D. Groot and P. Warren, Dissipative particle dynamics: bridging the gap between atomistic and mesoscopic simulation, J. Chem. Phys. **107**, 4423 (1997).

[37] M. Borkovec and G. J. M. Koper, Ising models of polyprotic acids and bases, J. Phys. Chem. **98**, 6038 (1994).

[38] A. Katchalsky and P. Spitnik, Potentiometric titrations of polymethacrylic acid, J. Polym. Sci. **2**, 432 (1947).

[39] J. C. Leyte and M. Mandel, Potentiometric behavior of polymethacrylic acid, J. Polymer Sci. **2**, 1879 (1964).

[40] J. L. Garcés, S. Madurga, C. Rey-Castro, and F. Mas, Dealing with long-range interactions in the determination of polyelectrolyte ionization properties. Extension of the transfer matrix formalism to the full range of ionic strengths, J. Polymer Sci. B **55**, 275 (2017).

[41] Z. Ou and M. Muthukumar, Entropy and enthalpy of polyelectrolyte complexation: Langevin dynamics simulations, J. Chem. Phys. **124**, 154902 (2006).

[42] M. A. Trejo-Ramos, F. Tristán, J. L. Menchaca, E. Pérez, and M. Chávez-Páez, Structure of polyelectrolyte complexes by Brownian dynamics simulation: Effects of the bond length asymmetry of the polyelectrolytes, J. Chem. Phys. **126**, 014901 (2007).

[43] M. Goswami, J. M. Borreguero, P. A. Pincus, and G. Sumpter, Surfactant-mediated polyelectrolyte self assembly in a polyelectrolyte-surfactant complex, Macromolecules **48**, 9050 (2015).

[44] C. Meng and A. Rudin, Relationship between the hydrodynamic radius and the radius of gyration of a polymer in solution, Makromol. Chem., Rapid Commun. **2**, 655 (1981).

[45] W. M. Kulicke and C. Clasen, *Viscosimetry of Polymers and Polyelectrolytes* (Springer, Berlin, 2004), Chap. 5.

[46] J. Flory, *Principles of Polymer Chemistry* (Cornell University Press, Ithaca, New York, 1953), p. 611.